BEHAVIOUR OF COMPOSITE BEAMS UNDER NEGATIVE BENDING AND AXIAL TENSION

George Vasdravellis
Post-doctoral Research Fellow
University of Western Sydney
Sydney, Australia
E-mail: g.vasdravellis@uws.edu.au

Brian Uy
Professor
Head of School of Engineering
University of Western Sydney
Sydney, Australia
E-mail: g.vasdravellis@uws.edu.au

Ee Loon Tan
Lecturer
University of Western Sydney
Sydney, Australia
E-mail: g.vasdravellis@uws.edu.au

Brendan Kirkland
PhD candidate
University of Western Sydney
Sydney, Australia
E-mail: g.vasdravellis@uws.edu.au

1. ABSTRACT

Το παρών άρθρο εξετάζει τη συμπεριφορά σύμμικτων δοκών υποκείμενες σε συνδυασμό αρνητικής ροπής και αξονικού εφελκυσμού. Αρχικά παρουσιάζονται τα αποτελέσματα πειραματικών δοκιμών στο εργαστήριο του πανεπιστημίου του Δυτικού Σίδνεϋ (Αυστραλία) σε έξι σύμμικτες δοκούς υπό την επίδραση διαφόρων επιπέδων αξονικής δύναμης και κάμψης. Οι δοκοί φορτίστηκαν εώς την τελική τους αστοχία και καταγράφηκε το διάγραμμα αλληλεπίδρασης ροπής-αξονικής δύναμης, ενώ έγιναν συγκρίσεις με τη μέθοδο πλαστικής ανάλυσης της διατομής. Στη συνέχεια, χρησιμοποιήθηκε το πρόγραμμα ABAQUS για τη δημιουργία ενός τρισδιάστατου μοντέλου πεπερασμένων στοιχείων, ικανό να προσομοιώσει τη συμπεριφορά των σύμμικτων δοκών με αποδεκτή ακρίβεια εώς την κατάσταση αστοχίας. Το μοντέλο χρησιμοποιήθηκε για να γίνουν παραμετρικές αναλύσεις σε δοκούς διαφόρων ανοιγμάτων και γεωμετρίας, ώστε να γενικευτούν τα αποτελέσματα. Τέλος, μία εξίσωση διαστασιολόγησης προτάθηκε για το σχεδιασμό στην πράξη σύμμικτων δοκών υπό συνδυασμένη καταπόνηση.

2. INTRODUCTION

Composite steel-concrete beams are used in many types of structures, including steel framed buildings, bridges, stadiums and car parks. Composite beams are being increasingly used in situations where combinations of bending, shear and axial force may be introduced

into the beam. This may occur via the installation of post-tensioning cables; by the inclination of the beam such as in stadia or bridge approaches; in cable-stayed bridges; or by the necessity to transfer diaphragm forces from the floor plate into the shear core of a building. However, modern steel and composite structural codes, including Eurocode 4 [1], Australian codes AS2327 and AS5100 [2, 3] and American AISC [4], currently do not address the effects of combined actions in composite beams. The ultimate capacity of steel-concrete composite beams under the combined effects of axial tension and negative bending moment is investigated in the present study. Firstly, details of an experimental investigation into composite beams under combined axial tension and negative bending are provided. Six composite beams of identical cross-section were tested in the laboratory of the University of Western Sydney under different combinations of tension and bending and the plastic capacities and failure modes were identified. The results were compared with the capacities provided by rigid plastic analysis through the composite section and reasonable agreement was found. The last section of the paper provides details of an extensive numerical study using the finite element method. The tested beams were modelled by a nonlinear finite element model in the ABAQUS commercial software. The three-dimensional model was compared against experimental results and found to be capable of simulating the inelastic behaviour of the composite beams with efficiency and to trace the failure modes up to ultimate load levels.

3. EXPERIMENTAL PROGRAMME

A total of six steel-concrete composite beams with identical cross-sections were tested in the Laboratory of the University of Western Sydney. All specimens were constructed with a 600mm wide and 120mm deep concrete slab connected to a 200UB30 steel section. The beam-slab connection was achieved through 19mm diameter, 95mm long headed shear studs welded in a single line along the centre of the top flange of the steel beam. The shear stud number was calculated in order to provide with full shear connection between the concrete slab and the steel beam. A group of 3 studs was welded to the ends of each of the beams to reduce slip and ensure full utilization of the reinforcing bars. Longitudinal and transverse reinforcement was placed in the concrete slab. The composite cross section for all specimens and a plan view of a typical specimen showing the shear stud and reinforcement arrangement is shown in *Fig. 1*.

The beam section was selected to be a class 1 (or plastic) section in order to be capable of achieving plastic rotations without being susceptible to premature local buckling [1, 2]. This was achieved by imposing the code limits to the slenderness of the steel beam flange and web. Attention should be paid in a composite section as the depth of the plastic neutral axis usually is considerably larger than half of the beam depth, as the steel reinforcement in the slab leads the plastic neutral axis to move near the top flange of the steel beam. Thus, the steel web should be classified taking into account the increased portion which is under compression [5].

As the universal beam bottom flange was subject to compression forces caused by the negative moment it was susceptible to lateral torsional buckling. Lateral buckling of the steel beam can cause premature failure of the composite beam and interruption of the test. As this was not under investigation in the present study, lateral movement and buckling of the steel beam was minimized by using a bracing system consisting of five sets of fly bracing located at the ends, quarter points and at the midspan. The distance of the bracing

was designed according to the current Australian structural code [2], which gives the maximum distances between two lateral restraints in order to eliminate the effects of distortional instabilities. Web stiffeners were welded to each side of the beam and the fly bracing was attached using grade 8.8 high tensile bolts. The connection to the slab also utilized grade 8.8 high tensile bolts which were cast in place. This arrangement can be seen in *Fig. 2***.**

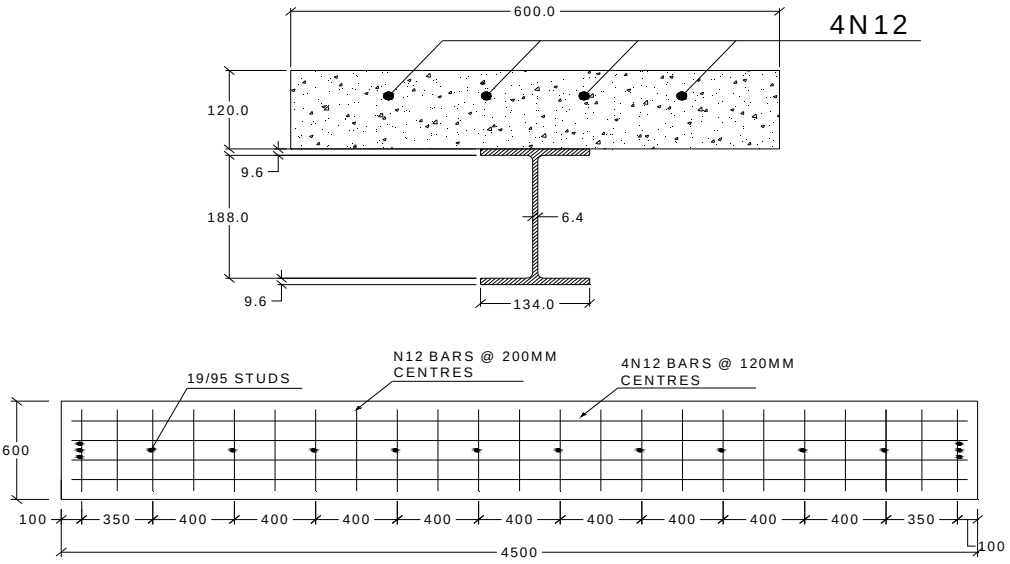

Fig. 1. Cross-section and plan view of the tested specimens

Material tests were performed prior to the tests in order to determine the actual strength and stiffness of steel and concrete. All materials were ordered from the same set, therefore it was assumed that the properties would be uniform. Tensile tests were performed on coupons cut from the steel web, flange and the reinforcing bars and the corresponding stress-strain laws were obtained. The concrete tests comprised of standard cylinder compression tests and flexural or splitting tests to determine the tensile strength of concrete according to Australian Standards [6].

Various measurement devices were employed to record the relevant parameters and to obtain the experimental behaviour of the beams. An automatic data acquisition system was employed to automatically record data from all measuring devices including load cells, strain gauges and linear potentiometers throughout the test. Strain gauges were used to measure strains of the steel beam and reinforcing bars and to determine at what load the components yield. Linear potentiometers were used for measuring the deflection of the beam and the interface slip. The test setup is shown in *Fig. 2*. A combination of load actuators was used in order to produce axial tension loads and bending moments in the composite beam specimens. The UWS testing laboratory has a test bed for testing specimens in axial loading consisting of two large universal columns with crossheads. To create the axial load two 800kN-160mm-stroke hydraulic actuators were used, thus capable of producing axial loads up to 1600kN in the composite beams.

Fig. 2. The test setup

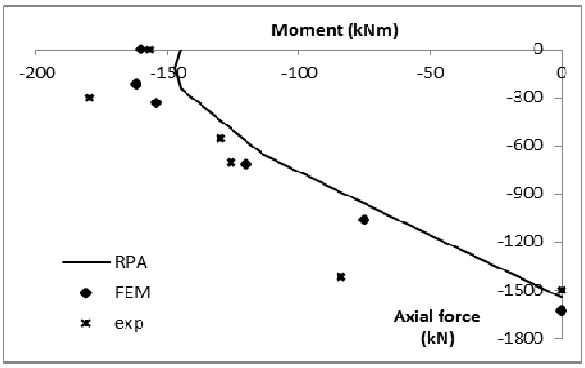

Fig. 3. Interaction diagram and comparison between experimental and analytical values

The six composite beams were tested under combined bending moment and axial tension and the ultimate strength achieved by each specimen was determined. The lateral torsional buckling of the compressive flange was prevented by the use of lateral restraints, thus the ultimate capacity of each beam was determined by one of the four possible failure conditions: 1) excessive yielding or fracture of the reinforcement, 2) local buckling of the compressive flange, 3) failure of the shear connection, or 4) ductile failure. The ductile failure mode is defined as the failure mode of a composite beam when none of the first three conditions is met and the beam deformations are excessive, while load applicators reach their maximum strokes. *Table 1* summarizes the failure modes of the six specimens.

An analytical calculation of the composite beam capacities was also conducted by means of rigid plastic analysis (R.P.A.) within the section. In this analysis only the steel parts (reinforcement bars and steel beam section) of the composite section are considered to contribute to the section capacity, while the concrete in tension is neglected. For comparison purposes with the experimental values, no partial safety factors have been used and the average yield strength resulted from the material tests were assumed for the steel parts.

The values obtained by the tests and those calculated by R.P.A. are plotted in the same graph in the interaction diagram of *Fig. 3*. This is the lower left quadrant of the complete moment-axial force interaction diagram of a composite section. It is observed from the same graph that the experimental data points follow the same basic shape as the theoretical interaction diagram, but are greater in most cases including negative bending, combined negative bending and tension, and less than for the case of pure axial tension. The increase can partially be explained by the strain hardening of the steel components and ultimate strengths found to be greater than yield strengths in the tests. The decrease can be explained by premature failure of the shear connection during the test of beam CB6 which is not considered in the sectional analysis.

From the interaction diagram it can be concluded that the flexural strength of a composite section is not affected or is even slightly increased under the simultaneous action of a low axial tension up to about 20% of the ultimate axial strength of the composite beam. This is also shown by composite beam CB2 results which had an increase of about 6% over the negative moment capacity of CB1. For axial tensile load levels above the 20% of the

ultimate axial strength, the flexural capacity reduces in a linear manner as the axial tension is increased.

Furthermore, the experimental study has confirmed that sectional rigid plastic analysis is a reasonable assumption of ultimate design strength of composite beams under the effects of combined negative bending and axial tension. A rigid plastic analysis could be used for design of composite beams subject to these forces since it is fairly accurate and will produce a fairly conservative figure for composite beam strength under the combination of negative bending and axial forces.

Specimen	Loading	Failure mode
CB1	Pure negative bending	Buckling of compressive flange
CB2	Negative bending and mild axial tension	Buckling of compressive flange
CB3	Negative bending and moderate axial tension	Ductile failure
CB4	Negative bending and high axial tension	Reinforcement fracture
CB5	Negative bending and very high axial tension	Reinforcement fracture
CB6	Axial tension only	Shear connection failure

Table 1: Experimental failure modes

4. FINITE ELEMENT ANALYSES

The experimental program described in the previous sections provided data on the ultimate strength of composite beams under the combined effects of negative bending and various levels of axial tensile forces. Nevertheless, the test results regard only one specific composite section. In order to generalize the results and to study a broader range of sections, the finite element method has been employed. For this purpose, a three-dimensional finite element model was constructed in order to reproduce the tests on the composite beams. The model is relying on the use of the commercial software ABAQUS [7].

The concrete slab and the steel beam were modelled using eight-node linear hexahedral solid elements with reduced integration, namely C3D8R in ABAQUS. The reinforcing bars were modelled as two-node three-dimensional linear truss elements, T3D2. An overview of the finite element discretization is shown in *Fig. 4*. The fly bracing was modelled indirectly by applying boundary conditions which prevent lateral displacement at the same points on the beam compression flange as the fly bracings were located in the tests. Due to the symmetrical geometry and loading, only half of the beam was modelled, while appropriate boundary conditions were applied on the plane of symmetry. A schematic representation of the various modelling assumptions is depicted in *Fig. 4*.

For modelling the reinforcement in the slab the embedded element technique was employed. The embedded element technique in ABAQUS is used to specify an element or a group of elements that lie embedded in a group of host elements whose response will be used to constrain the translational degrees of freedom of the embedded nodes. In the present case, the truss elements representing the reinforcement are the embedded region

while the concrete slab is the host region. In addition, a contact interaction was applied in the beam-slab interface which did not allow separation of the surfaces after contact in order to prevent uplift. The node-to-surface contact with small sliding was used while the hard contact without friction was specified as the contact property.

The stress-strain laws resulting from the material tests were multi-linearized and used for the modelling of the steel parts of the beam and the reinforcing bars. The isotropic hardening law was used as the constitutive law for all steel parts of the model.

The concrete material stress-strain relationship was calibrated according to the values obtained from the concrete cylinder and splitting tests. The stress-strain curve for compression follow the formula proposed by Carreira and Chu [8], while the tensile behaviour is assumed to be linear up to the uniaxial tensile stress provided by the material test. Of the available concrete models in ABAQUS, the damaged plasticity model was preferred over the smeared cracked model. A spring model representation of shear studs is chosen to simulate the interface slip. The nonlinear spring element SPRING2 was adopted to connect a beam flange node with a slab node in the interface at the same positions where studs were welded on the specimen, as schematically shown in *Fig. 4*. The force slip law for the spring element is derived by the standard push-out tests on 19mm-diameter shear studs. The experimental curve was multi-linearized and defined as the force-slip law for the springs.

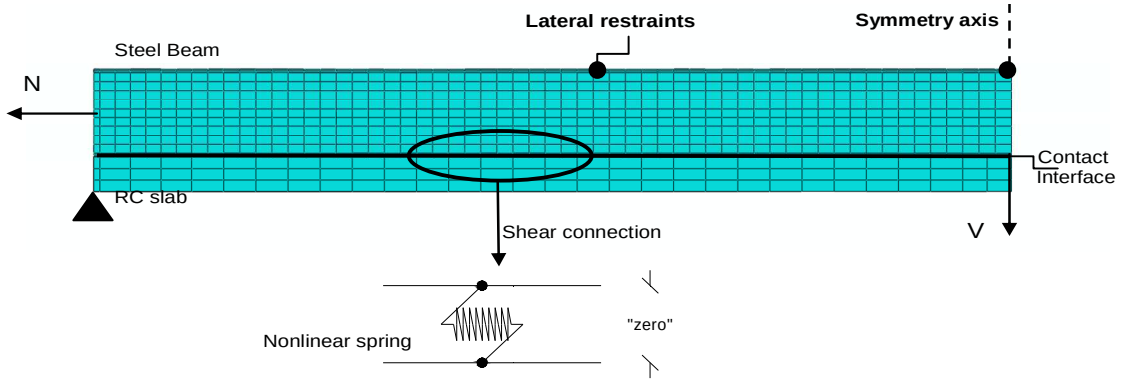

Fig. 4 The finite element model

Fig. 3 illustrates the resulting data in the M-N interaction diagram resulting from the tests, the RPA and the FE model. The FE points follow the same trend as the RPA analysis with a small over-prediction, which is expected mainly due to the strain hardening effects which are not present in the RPA. For intermediate axial load levels, as for specimens CB3 and CB4, the resulting points are in very good agreement, whereas there is some discrepancy observed for the CB5 and CB2 case. Further details regarding the assessment of the numerical model can be found elsewhere [9].

In order to generalize the results and to propose a reliable M-N interaction equation for design, a parametric study was conducted using a series of beams with different design parameters. More specifically, the span length was varied and accordingly the slab effective width and reinforcement ratio were designed for each parametric case according to current codes. Details on the design of the parametric beams are shown in *Table 2*.

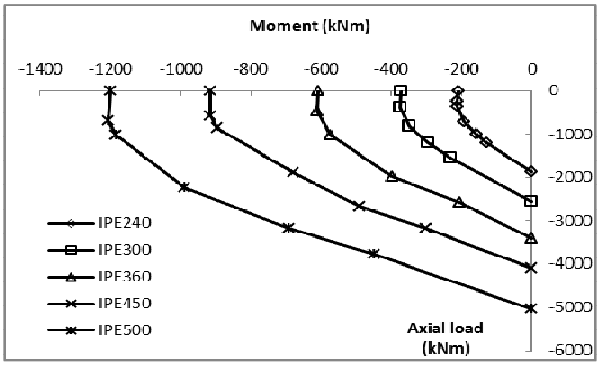

Fig. 5. Interaction diagram resulting from the parametric beams

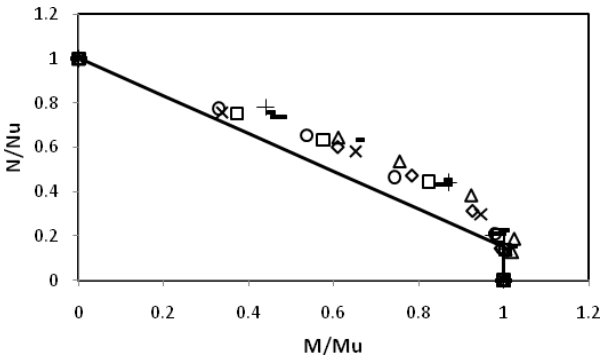

Fig. 6. Normalized interaction diagram and proposed design equation

Span (m)	q_{des} (kN/m)	M_{des} (kNm)	V_{des} (kN)	m/q	b_{eff} (mm)	A_s (mm^2)	Beam section	Shear studs (No/spacing in mm)
8	25.8	-117	96	1.22	1000	791	IPE240	14/307
12	25.8	-264	144	1.84	1500	1130	IPE300	20/315
16	25.8	-469	192	2.45	2000	1469	IPE360	24/347
20	25.8	-733	239	3.06	2000	1469	IPE450	24/434
24	25.8	-1055	287	3.67	2000	1808	IPE500	24/521

Table 2: Parametric beam design details

Fig. 5 plots the interaction data points resulting from the FE analyses of the five parametric beams with full shear connection in the same graph. The parametric analyses verify the shape of the interaction diagram for the fourth quadrant observed in the experimental beam. The main outcome is that the bending strength of a composite beam is not affected or is slightly increased in the presence of an axial tensile force up to 20% of the tensile strength of the composite section. In most cases the bending resistance with a low axial level of about 15-20% of Nu is slightly increased by 0.5-1.5%. For tensile axial loads greater than 20% of the plastic axial resistance the negative moment capacity is reduced almost linearly by increasing the axial tension in the beam.

The non-dimensional moment-axial force interaction data points for all parametric beams are plotted in *Fig. 6*. A design curve is superimposed on the analysis data points. Taking into account the various safety factors that are introduced in the practical design by all structural codes, the following design equation is proposed for the design of a composite beam under the combined effects of negative bending and axial tension

$$\frac{N}{N_U}+\frac{8}{10}\frac{M}{M_U}=1, \quad \text{for } \mathrm{N} \geq 0{,}20\mathrm{N}_\mathrm{U} \qquad (1)$$

$$M = M_U, \quad \text{for } \mathrm{N} < 0{,}20N_U \qquad (2)$$

where N and M are the design axial force and bending moment and N_u and M_u are the plastic axial and bending capacities of the composite beam, which can be calculated by

means of the rigid plastic analysis method, as described in various structural codes and is proven to be a reasonably conservative method.

5. CONCLUSIONS

The ultimate capacity of composite beams under the combined effects of negative bending and axial tension was investigated in this paper by means of both experimental and numerical studies. It was assumed that adequate lateral restraints are provided to the compression flange so that the beam is not susceptible to lateral torsional buckling. The experimental study has demonstrated that the negative moment capacity of composite beams is not affected or is even slightly increased when axial tension up to 20% of the axial plastic resistance is simultaneously acting in the composite section. For higher values of axial tension, the moment capacity is reduced almost linearly by increasing the tension level. Sectional rigid plastic analysis in accordance to current design codes has been proven to be reasonably accurate and to provide with plastic capacities which can be used in the design practice safely. The finite element analyses have confirmed the interaction curve shape for composite beams with a broader range of steel sections, span lengths and slab widths. Finally, a design formula has been proposed for composite beams subjected to a combination of negative bending moment and axial tensile loads. The design formula is the same for composite beams with full and partial shear connection and is based on the results of both the experimental study and the finite element analyses, while the design resistances are computed according to rigid plastic theory, in accordance to current structural codes.

6. REFERENCES

[1] Eurocode 4. Design of composite steel and concrete structures, part 1.1: general rules and rules for building. BS EN 1994-1-1: 2004. London (UK): British Standards Institution; 2004.

[2] Standards Australia. . Composite structures Part 1: Simply supported beams. AS 2327.1-2004. Sydney (Australia); 2004.

[3] Standards Australia. Bridge design, part 6: steel and composite construction. AS 5100.6-2004. Sydney (Australia); 2004

[4] ANSI/AISC 360-05. Specification for structural steel buildings. Chicago (IL, USA): American Institute of Steel Construction; 2005

[5] Johnson RP. Composite structures of steel and concrete. Volume 1: Beams, slabs, columns, and frames for buildings, 2nd ed., Oxford: Blackwell Scientific Publications, 1994

[6] Standards Australia. Methods of testing concrete. AS1012.9-1999. Standards Australia International Ltd

[7] ABAQUS user's manual, version 6.9. Hibbit, Karlsson & Sorenson. Pawtucket, RI, 2005

[8] CARREIRA D.J. and CHU K.H. "Stress-strain relationship for plain concrete in compression", *ACI Journal. Proceedings*, Vol. 82, No. 11, 1985, pp. 797-804.

[9] VASDRAVELLIS G., UY B., TAN E.L. and KIRKLAND B. "Ultimate strength of steel-concrete composite beams under negative bending and axial tension", *Journal of Constructional Steel Research. In Press*.